March, 1992] © *1992 The Chemical Society of Japan* *Bull. Chem. Soc. Jpn.*, ***65***, *761—770 (1992)* 761

Crystallization of Silica Gel in Alkaline Solutions. Characterization of SiO_2-X_2 and Other Crystalline Silicates by Comparing with Kenyaite

Haruto Muraishi
Faculty of Liberal Arts and Science, Kyushu Sangyo University,
2-3-1, Matsukadai, Higashi-ku, Fukuoka 813

(Received August 5, 1991)

Several hydrated alkali silicates, SiO_2–Y, SiO_2–X_2, and another silicate, form as intermediate products of the transformation of amorphous silica to quartz in alkaline solutions containing sodium and/or potassium salts at a temperature below 170 °C. SiO_2–X_2 ($M_2Si_{20}O_{41}\cdot xH_2O$, M=K, Na, x=8—10) usually appears after the formation of SiO_2–Y ($Na_2Si_{14}O_{29}\cdot xH_2O$, x=9—11), and can also be prepared directly from a solution with the pH adjusted to about 9.5 or from a solution containing potassium ion alone. The resulting SiO_2–X_2 materials are compounds of hydrated sodium-, potassium- and (sodium, potassium)-form silicates. Another silicate precipitates directly from the solutions with the pH adjusted to below 9.5 by use of sodium carbonate and sodium hydrogencarbonate, and the product is a hydrated sodium silicate, $Na_2Si_{22}O_{45}\cdot xH_2O$ (x=7—11). The structure and properties of this silicate are the same as that of natural kenyaite which is supposed to be a precursor of chert forming in evaporative alkaline lakes. These synthesized silicates have a layered structure and the interlayer alkali metal ions are exchanged by protons.

Quartz has been considered to be formed from a supersaturated solution of silicic acid or from amorphous silica over hundreds or thousands of years at temperatures above or below 100 °C. When mineralizers (such as alkalis and alkali metal salts), seed crystals, and some metal oxides are mixed in hydrothermal solutions, these added ions or foreign materials act as a catalyst for nucleation and crystal growth, and the crystallization is accelerated significantly.[1] The resulting intermediate phases, e.g., cristobalite and keatite, are usually one-component SiO_2 systems. When the mineralizer is added at lower temperature and lower pressure (e.g., 100—200 °C, 1—15 atm), a part of the mineralizer (such as alkalis) becomes incorporated into the intermediate products, which are binary or ternary systems such as hydrous alkali silicates. It is suggested that the appearance of intermediates results in a lowering of activation free energy for the transformation of amorphous silica to quartz. The reaction paths which were observed at lower temperatures are shown below:

$$\text{am. SiO}_2 \longrightarrow \text{SiO}_2\text{–X} \longrightarrow \text{cristobalite} \longrightarrow \text{quartz}$$

(Heydemann, 1964)[2]

$$\begin{tikzcd}
 & \text{SiO}_2\text{–X}_1 \arrow[r] & \text{SiO}_2\text{–X}_2 \arrow[dr] & & \\
\text{am. SiO}_2 \arrow[ur] \arrow[dr] & & & \text{cristobalite} \arrow[r] & \text{quartz} \\
 & \text{SiO}_2\text{–Y} \arrow[uur] \arrow[urr] & & &
\end{tikzcd}$$

(Mitsyuk *et al.*, 1976)[3]

$$\begin{tikzcd}
 & \text{SiO}_2\text{–Y} \arrow[d] \arrow[dr] & & \\
\text{am. SiO}_2 \arrow[ur] \arrow[r] & \text{SiO}_2\text{–X}_2 \arrow[r] & \text{cristobalite} \arrow[r] & \text{quartz}
\end{tikzcd}$$

(Muraishi, 1989)[4]

$$\text{soluble SiO}_2 \longrightarrow \text{magadiite} \longrightarrow \text{kenyaite} \longrightarrow \text{quartz}$$

(Euguster, 1967, Beneke and Lagaly, 1983)[5,6]

where am. SiO_2 represents amorphous silica. SiO_2–X is not a phase in the binary system SiO_2–H_2O, but always contains some alkali ions. SiO_2–X_1, SiO_2–X_2, and SiO_2–Y are hydrous alkali silicates. It is difficult to determine the exact chemical formula since the included cations are easily exchanged by protons. For these reasons, these silicates are usually abbreviated to "SiO_2–X_2, SiO_2–Y, etc." as described above.

In a previous paper,[4] it was reported that SiO_2–X, SiO_2–Y, and SiO_2–X_2 appeared as intermediates in the crystallization of amorphous silica to quartz in alkali solutions containing sodium and potassium salts at 100 to 180 °C. SiO_2–Y is magadiite ($Na_2Si_{14}O_{29}\cdot xH_2O$) which has been considered to be a precursor of inorganic bedded cherts.

In this study, the crystallization of amorphous silica was performed mainly in solutions containing sodium carbonate and sodium hydrogencarbonate; these alkalis were the immediate alkali sources in an alkali lake, e.g., Lake Magadi, in which various alkali silicates were produced in nature. When the mixture of sodium carbonate and sodium hydrogencarbonate was used as a mineralizer, SiO_2–Y, SiO_2–X_2, and another hydrous silicate (tentative name: SiO_2–Z) appeared. The natures of SiO_2–X_2 and SiO_2–Z were determined and compared with that of kenyaite, which was discovered at Lake Magadi, Kenya.

Experimental

General Procedure. The crystallization of amorphous silica was followed as a function of time at a constant temperature. In a typical run, 0.3 g of silica (Wako's silica gel Q-22, through 200 mesh) was dispersed in 7.5 ml of alkali solution containing Na_2CO_3 and $NaHCO_3$ corresponding to one molar concentration of Na. The suspension was placed in a 15 ml Teflon bottle, and the bottles were put in a stainless steel vessel with distilled water to adjust the pressure in the bottle to that in the vessel. After the run, the suspension was filtered off, washed with distilled water, and dried at room temperature. The washing was stopped when the filtrate reached about pH 10, since the intermediate silicates had ion exchange ability, and lost the included alkali metal ions when washed with a large excess of water.

Analyses. The products were examined using an X-ray powder diffractometer with Cu *Kα*-radiation. The chemical composition of the products was determined by a gravimetric method for silica and by an atomic absorption method for Na and K. The titration curve of the silicate suspension with 0.1 M HCl (1 M=1 mol dm^{-3}) was obtained in the following way. 0.5 g of silicate was dispersed in 50 ml of distilled water in a Teflon beaker, and the suspension was stirred. HCl was added by using an automatic titrator at a rate of 1.0 ml h^{-1}. The thermal behavior of the products was measured by differential thermal analysis (DTA) and thermo gravimetric analysis (TG) at a heating rate of 10 °C min^{-1}.

Results and Discussion

Formation Conditions of Intermediary Silicates. Effect of NaCl Concentration on the Formation of Intermediate Phases: As has been partly described in a previous paper,[4] when various amounts of sodium chloride were added to suspensions containing amorphous silica and KOH, three types of pathways for the transformation of amorphous silica to quartz were observed and could be summarized as follows.

(1) When there was no salt or trace amount of sodium chloride in a 1% KOH solution, the transformation was described as,

$$\text{am. SiO}_2 \longrightarrow \text{SiO}_2\text{-X} \longrightarrow \text{cristobalite} \longrightarrow \text{quartz}$$

(2) When the concentration of sodium ion was less than that of potassium ion, the reaction was as follows.

$$\text{am. SiO}_2 \longrightarrow \text{SiO}_2\text{-X}_2 \longrightarrow \text{cristobalite} \longrightarrow \text{quartz}$$

(3) In the case where the concentration of sodium ion was relatively high, the reaction path was

$$\text{am. SiO}_2 \longrightarrow \text{SiO}_2\text{-Y} \longrightarrow \text{SiO}_2\text{-X}_2 \longrightarrow \text{cristobalite} \longrightarrow \text{quartz}$$

The increase in the concentration of NaCl resulted in the appearance of silicates containing much more sodium ion. These results are summarized in Fig. 1.

As shown in Fig. 1, the addition of sodium chloride also brought about a reduction of the period of time before the beginning of quartz formation, and an increase in the lifetime of cristobalite. It was thought that cristobalite was stabilized when it included excess NaCl.

Effect of Sodium and Potassium Ions on the Transformation to Quartz: The crystallization of amorphous silica was further examined in alkali solutions containing various amounts of Na$^+$ and K$^+$ ion to determine the effect of the kinds of cations on the transformation. Solutions with various Na$^+$/K$^+$ ratios were prepared by use of NaOH and KOH as alkali sources and NaCl and KCl as salts; the sum of the moles of Na$^+$ and K$^+$ ions in the solutions was held constant at

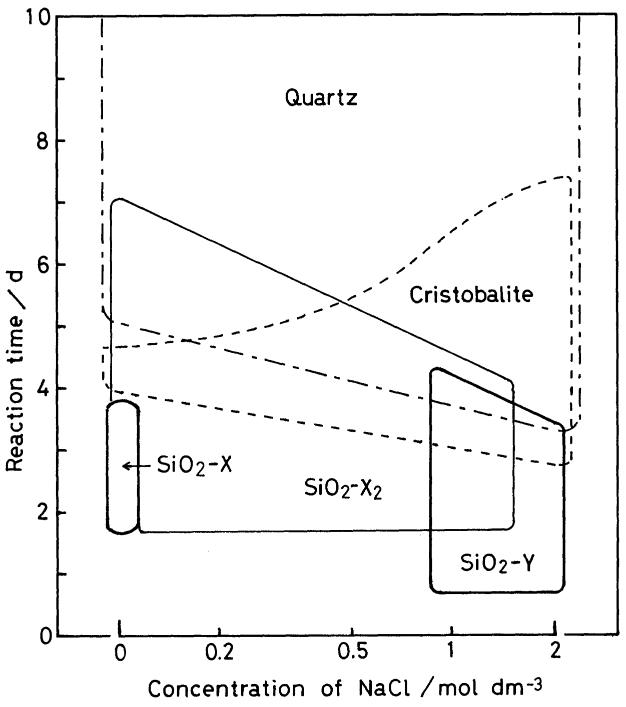

Fig. 1. Crystallization of amorphous silica in 1% KOH solutions containing various amounts of NaCl at 160 °C as a function of reaction time.

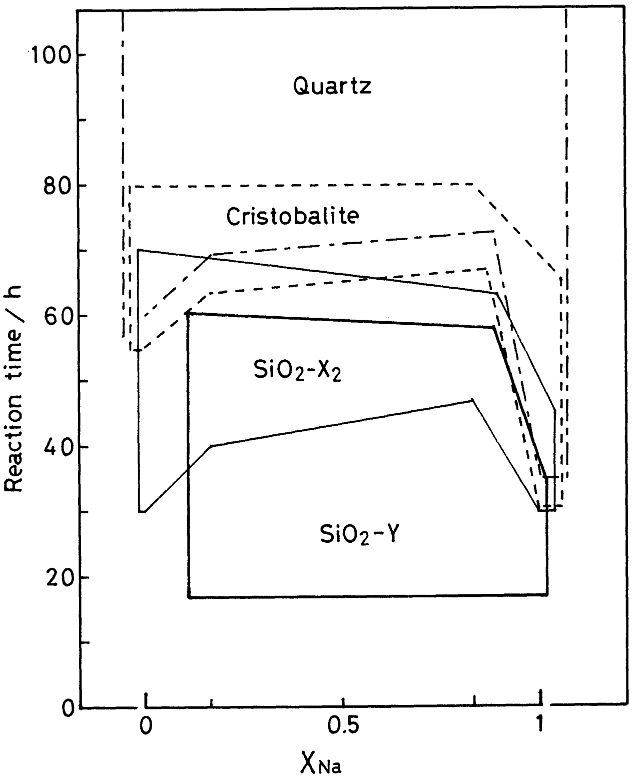

Fig. 2. Crystallization of amorphous silica in alkaline solutions containing Na and K at 160 °C as a function of reaction time. X_{Na}: Atomic ratio of Na/(Na+K).

1.2 mol dm^{-3}. As shown in Fig 2, SiO_2–X_2 was formed as an intermediate silicate in the alkali solution containing KOH and KCl. For the solution containing both Na^+ and K^+, or Na^+ alone, SiO_2–Y and SiO_2–X_2 appeared successively. When the alkali solution containing NaCl and NaOH was used, the rate of transformation to quartz was much faster than that of the other solutions.

Chemical analysis showed (as will be described in the following section) that SiO_2–X_2 existed in various forms such as sodium-, potassium-, and (sodium, potassium)-form silicates. In contrast with SiO_2–X_2, SiO_2–Y precipitated only as a sodium form silicate. The chemical composition of the resulting SiO_2–X_2 varied with the ratio of Na/K in the solution. In order to determine the affinity of sodium and potassium for SiO_2–X_2, two subsequent experiments were carried out to determine: (1) the ratio of Na/K incorporated in the precipitation in the course of the crystallization of amorphous silica to quartz via SiO_2–X_2 and (2) the relationship between the composition of the starting solutions and the composition of well-crystallized SiO_2–X_2. The former study was run in equimolar solutions of Na^+ and K^+. The solid phase was taken out at regular time intervals and analyzed. The latter study was run in solutions with various Na^+/K^+ ratios. When the silicate generated was mostly SiO_2–X_2, the resulting solid phase was taken out and analyzed.

The results of these experiments are summarized as follows.

(1) In the initial stage of the growth of SiO_2–X_2, the solid phase, which consisted of the silicate generated and unreacted amorphous silica, preferentially took up potassium ion from the solution as shown in Fig. 3. In the following stage, sodium ion was slowly taken up with the growth of SiO_2–X_2. When SiO_2–X_2 completely crystallized, the ratio of Na/K in the products was about 1.8; the apparent chemical formula of the products is represented by $Na_{1.3}K_{0.7}Si_{18}O_{37}\cdot xH_2O$. In a further stage, both sodium and potassium ions included in the products were gradually released with the transformation of SiO_2–X_2 to quartz.

(2) The chemical composition of the resulting well-crystallized SiO_2–X_2 showed that the ratio of Na/K in the products was always larger than that of the starting solution. For example, when the ratios of Na/K in the solutions were 3, 1, and 0.33, those of the products were 6.7, 1.8, and 0.45, respectively. It was therefore presumed that potassium ions acted effectively as a core for nucleation in the initial crystallization stage, and in a further stage, sodium ions became incorporated into the crystal as the principal constituent.

Effect of Solution pH on the Crystallization of Amorphous Silica: The processes of the transformation of amorphous silica to quartz were observed as a function of solution pH. The solutions were adjusted to a pH range of about 8—12 using sodium carbonate and sodium hydrogencarbonate in various proportions, and the suspensions of silicate were prepared at a definite molar ratio of $SiO_2/Na=1/1.74$. Sodium carbonate and sodium hydrogencarbonate were the chief components of an alkaline brine in Lake Magadi,[7] in which magadiite and kenyaite have been found.

Figure 4 illustrates a log-log plot of hydrogen ion concentration of the starting solution against reaction time. In this figure, the single line shows the time of the first appearance of the intermediate phases, the double line shows the time necessary for 100% conversion to quartz, and the zone between the broken line and the

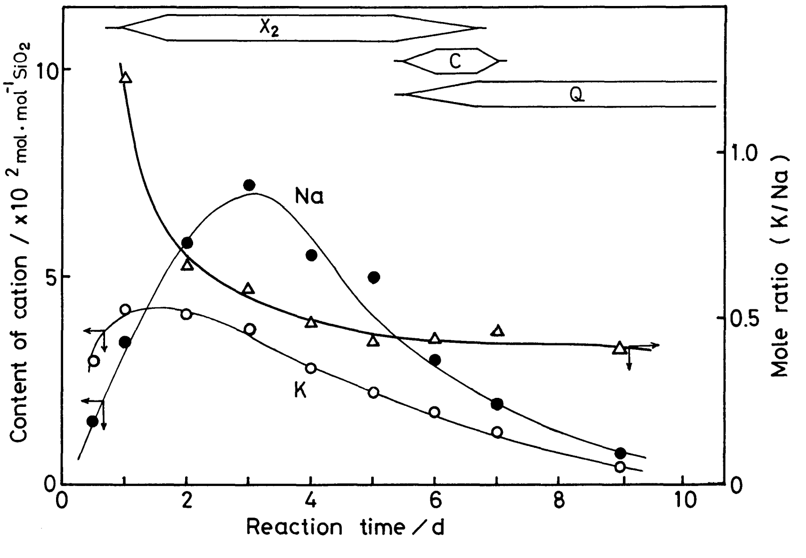

Fig. 3. Change of the content of Na and K in the intermediate products with the crystallization of amorphous silica to quartz. Alkali source: the mixture of Na_2CO_3 and $NaHCO_3$, and K_2CO_3 and $KHCO_3$. Concentration of alkali: 1 mol dm^{-3}.

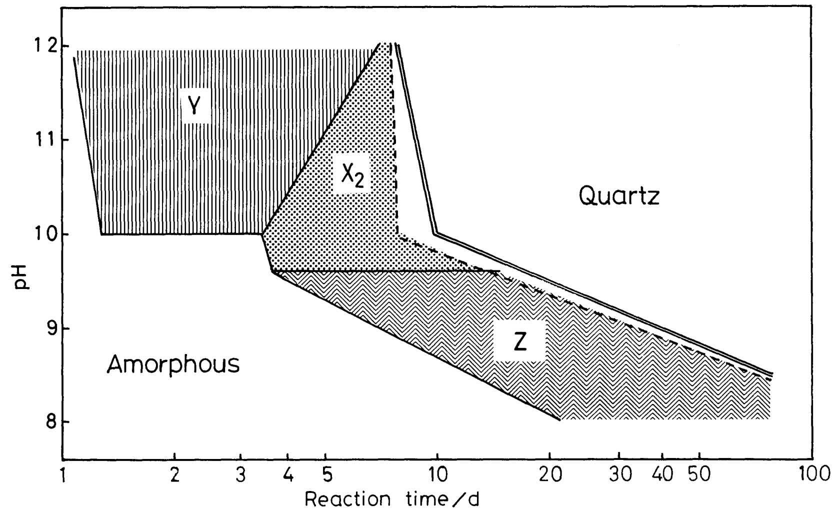

Fig. 4. Rate of crystallization of amorphous silica to quartz in the solution with changing pH. Alkali souce: a mixture of Na_2CO_3-$NaHCO_3$. Concentration: 1 mol dm^{-3}. Temp: 160 °C.

double line shows the range in which some phases (intermediate silicates, cristobalite and quartz) coexisted.

It was found that the pH dependence of the time necessary for 100% conversion to quartz drastically changed at a solution pH of about 10. Below about pH 10, the time t' necessary for 100% conversion to quartz was significantly dependent on the pH values of the solution; the relation between the time t' for complete conversion into quartz and the pH of the starting solutions was represented by a simple equation as $\log t' = -A\ \mathrm{pH} + B$ ($A=0.58$ and $B=6.85$). When the pH of the solution was above 10, conversion was almost independent of the pH. If the rate of the conversion to quartz were governed by the dissolved silica concentration in the solutions, the time t' would be observed as a function of pH in the solutions above pH 9, and below pH 9 it would be almost constant, as can be seen from the solubility curve of silica.[8] Actually, however, it was found that the time t' was governed by the species of intermediate products and their stabilities in the solutions.

The pathways for the transformation of amorphous silica to quartz also changed at a solution pH of 10. This crystallization can be represented by the following conversion.

(above pH 10)
am. $SiO_2 \longrightarrow SiO_2$-Y $\longrightarrow SiO_2$-$X_2 \longrightarrow$ cristobalite $\longrightarrow$ quartz

(at about pH 9.5)
am. $SiO_2 \longrightarrow SiO_2$-$X_2 \longrightarrow$ cristobalite $\longrightarrow$ quartz

(below pH 9.5)
am. $SiO_2 \longrightarrow SiO_2$-Z $\longrightarrow$ cristobalite $\longrightarrow$ quartz

When sodium carbonate and sodium hydrogencarbonate, or sodium hydrogencarbonate alone were used as alkali sources, a crystalline hydrous sodium silicate (tentatively named SiO_2–Z) was formed directly from amorphous silica. A well-crystallized SiO_2–Z could be obtained in the solutions with lower pH, such as the solution containing both 0.1 M Na_2CO_3 and 0.8 M $NaHCO_3$. When potassium carbonate–hydrogencarbonate was used as an alkali source, SiO_2–Z did not form.

In a further experiment, the effect of the amount of silica on the formation of the intermediate phases was investigated in solutions adjusted to various pHs in a manner similar to that described above. With an increasing molar ratio of SiO_2/Na in the suspension, the boundary between the three kinds of intermediate silicates formed shifted to a higher pH value compared to Fig. 4. For example, when the molar ratio of SiO_2/Na in the suspension was 3.3/1 adding excess silica, SiO_2–Z appeared below pH 10.5.

These results can be summarized as follows. SiO_2–Y was preferentially formed in a higher pH solution with a lower SiO_2/Na ratio. SiO_2–Z was preferentially formed in a lower pH solution with a higher SiO_2/Na ratio. SiO_2–X_2 was usually generated between the two speculated stability fields.

Properties of Intermediate Phases. Chemical Composition of Intermediate Silicates: As is shown in Fig. 2 and Fig. 4, SiO_2–X_2 was formed through two pathways: One was through SiO_2–Y, and the other was directly from amorphous silica. SiO_2–Y was formed only as a sodium silicate, but the resulting SiO_2–X_2 materials were alkali silicates containing sodium, potassium, or both sodium and potassium. The chemical composition varied with the composition of the starting hydrothermal solutions including sodium and potassium and also with the reaction temperature as shown in Table 1. The apparent chemical formula of

Table 1. Chemical Composition of SiO_2–X_2 Prepared under Various Conditions

Run No.	Preparation conditions	Composition of medium solution (molar ratio) Na	/ K	/ SiO_2	/ OH^-	/ H_2O	Atomic ratio of products Na	/ K	/ Si
[X_2 produced via Y]									
1	KOH–NaCl, 170 °C–20 h	0.90	0.32	1	0.32	100	1.57	0.32	22
2	KOH–NaCl–KCl, 170 °C–25 h	0.90	1.22	1	0.32	100	1.20	0.76	22
3	NaOH, 150 °C–18 d	0.12	—	1	0.12	6	1.93	—	22
[X_2 prepared directly from amorphous silica]									
4	KOH, 125 °C–2.5 m	—	0.22	1	0.22	8	—	1.83	22
5	KOH–KCl, 170 °C–25 h	—	2.12	1	0.32	100	—	1.91	22
6	Na_2CO_3–$NaHCO_3$, 160 °C–5.5 d	1.06	—	1	(pH 9.5)	60	1.85	—	22

Table 2. Chemical Composition of SiO_2–Z Prepared from Solutions Containing Na_2CO_3 and $NaHCO_3$ in Various Proportions

Run No.	Synthesis conditions[a)]		Atomic ratio of products Na	/ Si
1	Na_2CO_3–$NaHCO_3$ 160 °C–10 d	(1+1)	2.40	22
2	Na_2CO_3–$NaHCO_3$ 160 °C–14 d	(1+2)	2.26	22
3	Na_2CO_3–$NaHCO_3$ 120 °C–2 m	(1+2)	2.05	22
4	Na_2CO_3–$NaHCO_3$ 160 °C–16 d	(1+4)	1.84	22

a) "(*a*+*b*)" represents the ratio of *a* 0.5 M-Na_2CO_3 and *b* 1 M-$NaHCO_3$ used for preparation of the medium solutions.

SiO_2–X_2 was represented by $(Na_{2-y}, K_y)Si_{21}O_{43}\cdot xH_2O$–$(Na_{2-y}, K_y)Si_{24}O_{49}\cdot xH_2O$ for the products through SiO_2–Y, and by $(Na_{2-y}, K_y)Si_{17}O_{35}\cdot xH_2O$–$(Na_{2-y}, K_y)Si_{23}O_{47}\cdot xH_2O$ (where $0<y<2$, $x=8$—10) for the products formed directly as shown in Table 2. The most probable chemical formula obtained from the mean values of the sodium form of SiO_2–X_2 was represented as $Na_2Si_{20}O_{41}\cdot xH_2O$.

SiO_2–Z appeared only as a hydrous sodium silicate like SiO_2–Y, and the Na^+ content of the synthesized material tended to increase with an increase in the pH of the solution. The chemical composition of the products was $SiO_2/Na_2O=18.3$—23.9. The most probable chemical formula of SiO_2–Z was represented as $Na_2Si_{22}O_{45}\cdot xH_2O$. The amount of cations incorporated into a silicate is known to be directly proportional to the amount of negative charge in its interlayer. For SiO_2–Z and also SiO_2–Y, the alteration in the amount of Na with pH would be interpreted by the following equation.

$$\geqslant\text{Si-OH} + OH^- \longrightarrow \geqslant\text{SiO}^- + H_2O$$

When OH^- ions are increased, the equilibrium is shifted to the right, and the negative charge on the interlayer surface of the silicate is increased, in addition to the amount of Na contained inside.

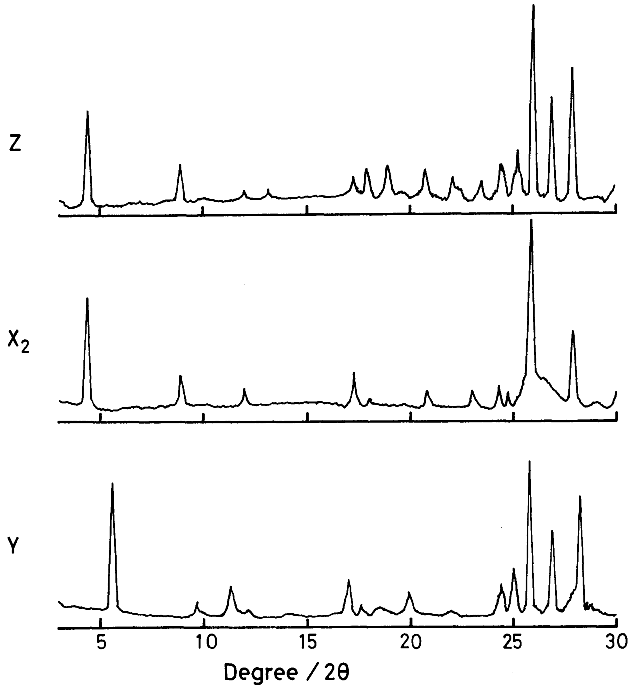

Fig. 5. X-ray diffraction patterns of SiO_2–Z, SiO_2–X_2, and SiO_2–Y.

X-Ray Diffraction Data: Fig. 5 shows X-ray diffraction patterns of typical intermediate silicates. Table 3 shows the *d*-values obtained from the X-ray diffraction powder patterns of some synthetic silicates studied in this experiment, a synthesized kenyaite reported by Beneke and Lagaly,[6)] and two known silicates, SiO_2–X_2 and natural kenyaite ($NaSi_{11}O_{20.5}(OH)_4\cdot 3H_2O$), reported by Mitsyuk[3)] and Eugster,[9)] respectively. All of the listed silicates had a similar basal spacing and some diffraction peaks having the same *d*-values. These silicates were classified in two groups by their X-ray diffraction powder patterns; group 1 (SiO_2–X_2, Na-form SiO_2–X_2 (Na–X_2), and K-form SiO_2–X_2 (K–X_2)) did not have the major reflections of $d=4.68$—4.70 Å ($I=20$—28), $d=3.32$—3.34 Å ($I=45$—70), $d=3.51$—3.53 Å ($I=10$—22), and 2.83 Å ($I=10$—12), shown by the group 2 silicates; group 2 consisted of natural kenyaite, SiO_2–Z, and synthesized kenyaite.

Table 3. X-Ray Powder Diffraction Data of SiO_2–X_2, Na-Form SiO_2–X_2(Na–X_2), K-Form SiO_2–X_2(K–X_2), Kenyaite, and SiO_2–Z

SiO_2–X_2 Mitsyuk[a]		Na–X_2 This work		K–X_2 This work		Synthetic kenyaite run 40 Y Beneke[6]		Natural kenyaite Eugster[5]		SiO_2–Z This work	
d/Å	I	d/Å	I	d/Å	I	d/Å	I	d/Å	I	d/Å	I
20.0	50	19.93	75	19.89	45	19.86	100	19.68	100	19.85	72
9.8	30	9.95	25	9.72	15	9.94	30	9.925	50	9.98	21
								7.775	2		
7.26	20	7.36	15	7.38	15			7.272	5	7.33	8
6.26	20							6.620	5	6.65	7
								5.637	7	5.64	7
						5.04	<10	5.142	12	5.15	10
5.01	50	4.97	20	4.86	15	4.98	10	4.965	35	4.96	20
						4.68	20	4.689	28	4.70	20
4.24	40	4.27	15			4.26	30	4.471	5	4.29	15
						3.93	20	3.954	10	3.96	10
3.79	30							3.754	5	3.77	6
		3.67	20	3.68	25	3.65	20	3.638	20	3.64	18
		3.61	20	3.61	20	3.51	10	3.525	22	3.53	22
3.45	100	3.44	100	3.44	100	3.43	70	3.428	85	3.43	100
						3.34	70	3.320	45	3.32	50
3.18	40	3.21	50	3.20	35	3.19	70	3.198	55	3.20	65
2.98	20	2.94	15	2.93	15	2.93	30	2.934	14	2.94	15
2.87	20					2.83	10	2.827	12	2.83	10
								2.652	3		
2.54	10							2.520	3	2.56	5
								2.482	3	2.49	5
								2.416	5	2.42	5
2.34	20							2.343	7	2.34	5
1.83	50	1.83	20	1.84	20	1.83	50	1.880	3	1.83	15

a) B. M. Mitsyuk et al., *Dokl. Akad. Nauk SSSR,* **209**, 926 (1973).

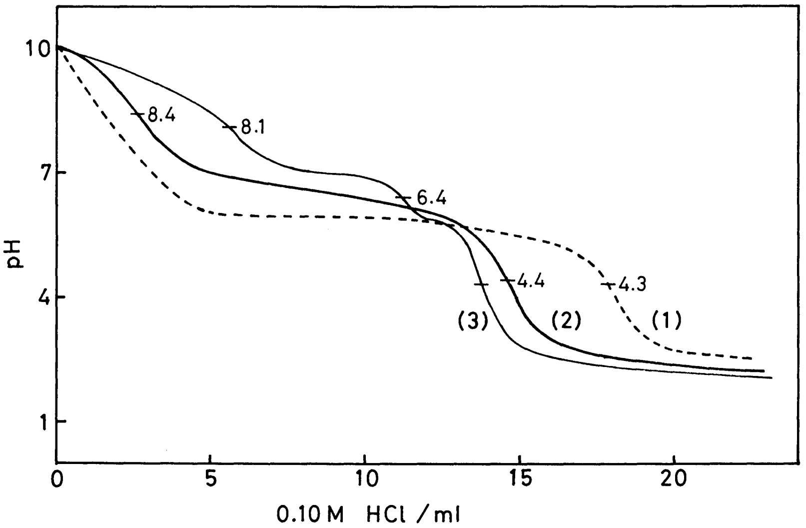

Fig. 6. Titration curves of sodium-form silicates suspensions with 0.1 M HCl solution. Suspension: 0.5 g of silicate/50 ml of water. Rate of addition of HCl: 1.0 ml h^{-1}. (1): SiO_2–Y, (2): SiO_2–Z, (3): SiO_2–X_2.

The diffraction pattern of SiO_2–Z was identical to that of natural kenyaite. The synthesized kenyaite without many small peaks appeared to be inferior to natural kenyaite in crystallinity.

Ion-Exchange Properties: Every hydrous silicate, SiO_2–Y, SiO_2–X_2, and SiO_2–Z, had a layered structure, and these interlayer alkali metal ions were easily exchanged by protons. Figure 6 shows the titration curves of these sodium-form silicate suspensions with diluted hydrogen chloride. The titration curves for both SiO_2–Y and SiO_2–Z corresponded to the curve for a monovalent weak base with only one pH jump at the

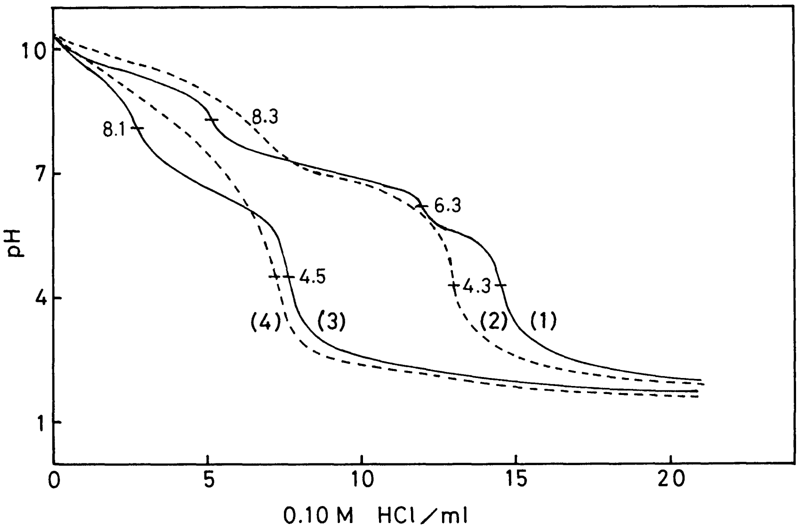

Fig. 7. Titration curves of (sodium, potassium)- and potassium-form SiO_2–X_2 suspensions. Suspension: 0.5 g of silicate/50 ml of water. Rate of addition of HCl: 1.0 ml h^{-1}. (1), (3): (Na, K)-form SiO_2–X_2; (2), (4): K-form SiO_2–X_2.

equivalence point, and at that point the interlayer sodium ions could be exchanged with protons up to 90 to 100% of the content.

Figure 7 shows the titration curves of (sodium, potassium)- and potassium-form SiO_2–X_2. SiO_2–X_2 behaved as a polyvalent weak base. The titration curves showed two or three pH jumps; one jump showed the pH value (pH=4.3—4.5) which corresponded to the equivalence point of SiO_2–Y and SiO_2–Z, and the others showed higher pH values (pH=6.4, 8.1—8.3) than those of these silicates. The exchange reaction of SiO_2–X_2 did not proceed completely; the amount of alkali metal ions which was released at the apparent equivalence point was only 40 to 90% of its content in the silicate.

The reasons why the cation exchange reaction of SiO_2–X_2 proceeded in multiple steps are thought to be as follows.

(1) There are several kinds of exchangeable sites with different energies, such as the silanol groups with distinct pK_a values on the interlayer surface.

(2) There are several kinds of alkali metal ions in different states, such as a naked cation fixed in the host framework and a hydrated cation existing in the interlayer of the silicate.

(3) There are several crystal phases with different cation/water contents.

In type (3), a step-by-step variation in chemical composition and in basal spacing should be observed with the ion exchange reaction, which has been observed for potassium ion exchange on hydrous titanium dioxide reported by Sasaki et al.[10] In our experiment, such variation was not observed even in many ion exchange runs.

For the reaction in type (2), it is believed that the alkali metal ions were not always replaced quantitatively by protons at the apparent equivalence point, since the naked cations fixed in the framework may be exchanged with difficulty, as was observed in our experiment.

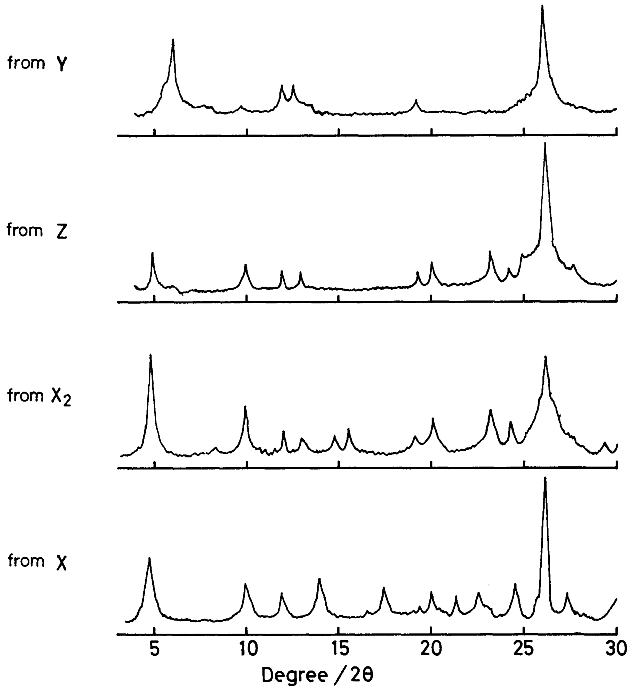

Fig. 8. X-ray diffraction patterns of H-form silicates derived from SiO_2–Y (Y), SiO_2–Z (Z), potassium-form SiO_2–X_2 (K–X_2), and SiO_2–X (X).

It was therefore presumed that the ion exchange with multiple steps was caused by a (1) or (2) type reaction.

When alkali metal ions were removed from potassium-form SiO_2–X_2 (K–X_2), the derived crystalline silicic acid (H–(K–X_2)) and its dehydrated silicic acid occasionally gave an X-ray powder pattern similar to that of SiO_2-X as shown in Fig. 8. On the other hand, Lagaly[11] has reported that the silicic acid $SiO_2 \cdot xH_2O$ obtained by dehydrating $H_2Si_8O_{17} \cdot xH_2O$ (prepared by the exchange of protons for potassium ions of synthesized $K_2Si_8O_{17} \cdot xH_2O$) was indeed SiO_2-X. It is of interest that SiO_2-X can be obtained through several pathways such as silicic acids obtained by the ion-exchange of two different alkali silicates and direct formation from KOH solution.

The crystalline silicic acids derived from sodium-form SiO_2-X_2 (Na-X_2), SiO_2-Z, synthesized kenyaite, and natural kenyaite had similar X-ray diffraction patterns, while these silicates before treatment were classified into two groups as described above. It is suggested that the three dimensional framework comprising the Si-O bond is very similar in these compounds.

Thermal Behavior. Figure 9 shows DTA diagrams for the dehydration of SiO_2-Y, SiO_2-Z, SiO_2-X_2, and synthesized kenyaite, which were prepared by the method of Beneke et al.[6]; reaction conditions: $SiO_2/H_2O/NaOH=6.75/1/0.11$ (by weight), and 150 °C-20 d. The DTA curve of SiO_2-Y indicated three endothermic peaks in the temperature range 120—190 °C. In this temperature range, about 90% of the total ignition loss was released. The DTA curves of SiO_2-Z, synthesized kenyaite and sodium-form SiO_2-X_2 had similar patterns. They indicated major peaks in the temperature range 60—145 °C, and a small endothermic peak above 280 °C. The first peak observed in the tempeprature range 60—85 °C was usually a doublet. The second peak observed in the temperature range 105—120 °C was a doublet in the case of SiO_2-Z, while those of synthesized kenyaite

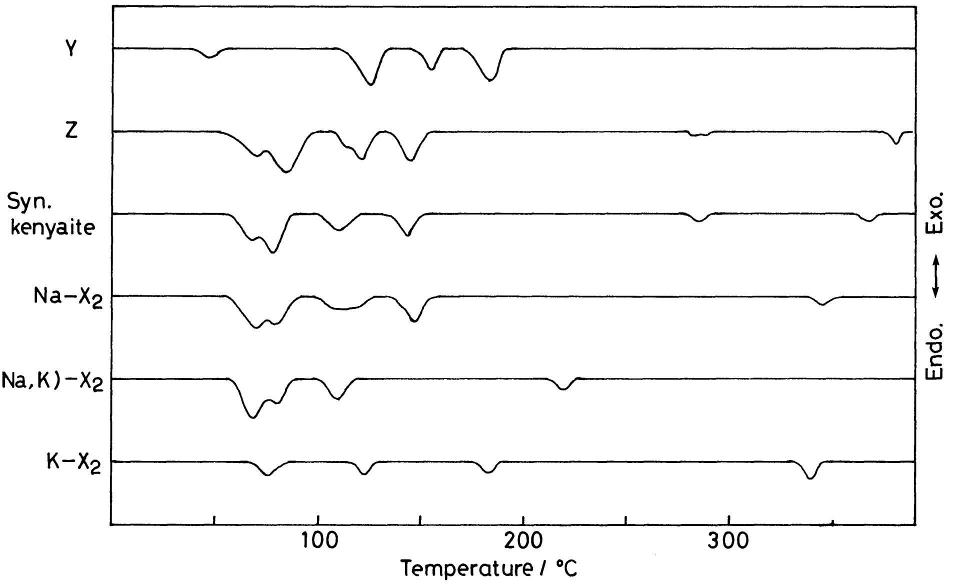

Fig. 9. DTA diagrams for the dehydration of SiO_2-Y (Y), SiO_2-Z (Z), synthesized kenyaite (syn. kenyaite), and sodium- and potassium-form SiO_2-X_2 (Na-X_2, (Na, K)-X_2, and K-X_2).

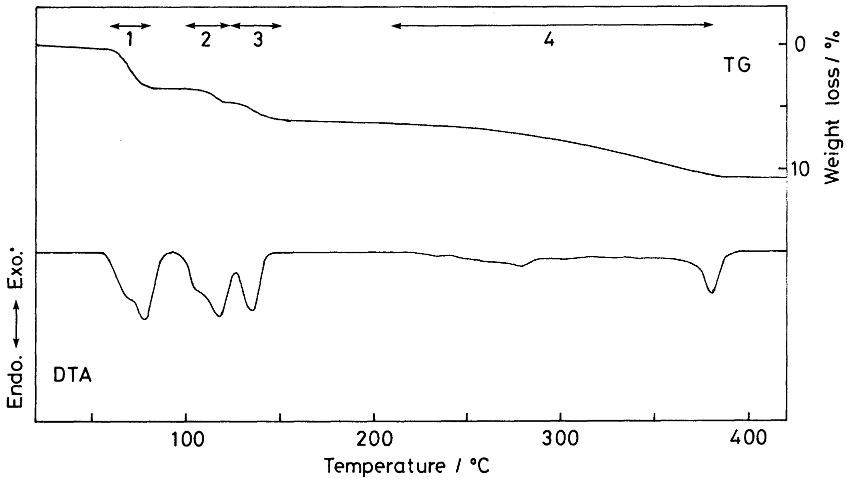

Fig. 10. TG and DTA curves of SiO_2-Z.

and sodium-form SiO_2–X_2 were very broad. The third peak observed in the range 135—145 °C was a singlet, and tended to shift position to lower temperatures with higher crystallinity.

Figure 10 shows the TG–DTA curves of SiO_2–Z. The TG curve indicated four well-defined stages corresponding to the endothermic peaks of DTA. In the case of synthesized kenyaite and sodium-form SiO_2–X_2, the TG curve indicated two stages, since stages 2, 3, and 4 represented in Fig. 10 were indistinguishable. It is suggested that the fine structure of the silicate layer of the two silicates was inferior to that of SiO_2–Z, whose X-ray diffraction data has already been considered.

The DTA curves of a series of SiO_2–X_2 containing sodium and potassium indicated a considerable change in the dehydration temperature with increasing potassium content. Potassium-form SiO_2–X_2 (K–X_2) gave four endothermic peaks that were very far apart over the temperature range 80—350 °C. The difference between Na–X_2 and K–X_2 may be due to either the difference of the affinity of water molecules with the cations or the difference in the fine structure of the silicate layer.

Table 4 shows the change of basal spacings and the transformation of K–X_2, Na–X_2, SiO_2–Z, synthesized kenyaite, and natural kenyaite with thermal treatment. A summary of these results is described as follows.

(1) The basal spacing of Na–X_2, K–X_2 and synthesized kenyaite was decreased by dehydration, while that of SiO_2–Z and natural kenyaite were little changed at a temperature of 200 °C or above even when the dehydration reaction was nearly complete. The fine structure in the silicate layer of SiO_2–Z and natural kenyaite was distinct from that of the other silicates.

(2) All sodium and potassium silicates listed in Table 4 were easily destroyed structurally by heating, and then recrystallized at a comparatively low temperature, compared with the silicic acids as described below. The recrystallization tended to proceed to the right in the following reaction.

$$\text{silicate} \longrightarrow \text{quartz} \longrightarrow \text{cristobalite} \longrightarrow \text{tridymite}$$

The conversion of silicates containing alkali metal ions was different from that of the transition of one component SiO_2;

$$\text{quartz} \longrightarrow \text{tridymite} \longrightarrow \text{cristobalite}.$$

The silica framework of H-form silicates derived from alkali silicates were not destroyed by heating even at 900 °C as shown in Table 5. The basal spacing was almost constant over the temperature range 400 to 900 °C.

Conclusions

(1) SiO_2–Y, SiO_2–X_2, and SiO_2–Z appeared as intermediate products in the course of the transformation of amorphous silica to quartz under hydrothermal conditions at 100—170 °C, when starting suspensions containing alkalis, and alkali metal salts were used.

Table 4. The Change of Basal Spacings and the Transformation of Silicates with Thermal Treatment

Temp	Basal spacings/Å				
°C	K–X_2	Na–X_2	Z	Synthetic kenyaite (Beneke[6)])	Natural kenyaite (Beneke[6)])
R.T.	19.9	19.9	19.9	19.7—19.9	19.7
200	18.8	18.8	19.8	17.7	19.6
400	18.8	18.8	19.9	17.7	—
600	17.7	18.8	19.8	17.7	—
700	C, Q	Q	Q	Q	—
800	T, C, Q	Q	Q	—	—
900	T, Q	Q	Q	—	—

a) K–X_2: potassium-form SiO_2–X_2, Na–X_2: sodium-form SiO_2–X_2, Z: SiO_2–Z. b) Q: quartz, C: cristobalite, T: tridymite.

Table 5. The Change of Basal Spacings of Crystalline Silicic Acids Derived from Alkali Silicates with Thermal Treatment

Temp	Basal spacings/Å				
°C	from K–X_2	from Na–X_2	from Z	from Synthetic kenyaite (Beneke[6)])	from Natural kenyaite (Beneke[6)])
R.T.	18.2	18.1	18.0	17.8	17.9
200	17.9	17.4	17.6	17.7	17.6
400	17.7	16.2	16.2	—	—
600	17.7	16.2	16.2	—	—
700	17.7	16.2	16.2	—	—
800	17.7	16.2	16.2	—	—
900	17.3	a)	a)	—	—

a) Unidentified crystal phase.

(2) The transformation of amorphous silica to quartz could be represented by the reaction paths as follows.

$$\begin{tikzcd}
 & SiO_2\text{–}Y \arrow[dd] \arrow[dr] & & \\
\text{am. } SiO_2 \arrow[ur] \arrow[dr] & & \text{cristobalite} \arrow[r] & \text{quartz} \\
 & SiO_2\text{–}X_2 \arrow[ur] & &
\end{tikzcd} \qquad [1]$$

$$\text{am. } SiO_2 \longrightarrow SiO_2\text{–Z} \longrightarrow \text{cristobalite} \longrightarrow \text{quartz} \qquad [2]$$

SiO_2–Y was formed only as a sodium-form hydrous silicate. SiO_2–Z was also a sodium-form silicate when both sodium carbonate and sodium hydrogencarbonate, or only sodium hydrogencarbonate were used as alkali sources. On the other hand, SiO_2–X_2 was formed as sodium-, potassium-, and (sodium, potassium)-form hydrous silicates.

(3) SiO_2–X_2, SiO_2–Z and kenyaite synthesized by Beneke et al. were closely similar in structure, while they were distinguishable from each other in several other properties. SiO_2–Z was the most crystallized silicate, compared with the others. SiO_2–X_2 and synthesized kenyaite appeared to be the silicates that were inferior to

SiO_2–Z in crystallinity. It is thought to be necessary to differentiate at least between SiO_2–X_2 and SiO_2–Z.

(4) SiO_2–Y is magadiite ($Na_2Si_{14}O_{29}\cdot xH_2O$) (as has been described in a previous paper[4]) and SiO_2–Z is kenyaite ($Na_2Si_{22}O_{45}\cdot xH_2O$), which are considered to be precursors of inorganic bedded chert formed in evaporative alkaline lakes.

(5) The mechanism of the formation of chert is thought to be as follows.

$$\text{soluble silica} \longrightarrow \underset{(SiO_2\text{–}Y)}{\text{magadiite}} \longrightarrow \underset{(SiO_2\text{–}Z)}{\text{kenyaite}} \longrightarrow \underset{(\text{quartz})}{\text{chert}} \qquad [3]$$

In our defined experimental conditions, this reaction did not proceed consecutively. If the consecutive reaction [3] were allowed to proceed, some alteration of experimental conditions, a drop of pH and the decrease of sodium concentration, should occur after the formation of magadiite.

(6) All of these synthesized silicates consisted of a layered structure and interlayer alkali metal ions were exchanged by protons. When SiO_2–Y and SiO_2–Z reacted with HCl, the titration curves for weak monoequivalent bases were obtained. For SiO_2–X_2 (Na–X_2, K–X_2, and (Na, K)–X_2), the titration curves were those of a weak polyequivalent base.

References

1) H. Muraishi and S. Kitahara, "Hydrothermal Reactions," ed by S. Somiya, Uchida Rokakuho, Tokyo (1986), Vol. 1, pp. 1—13.

2) A. Heydemann, *Beitr. Mineral. Petrol.,* **10**, 242 (1964).

3) B. M. Mitsyuk, L. I. Gorogodskaya, and A. I. Rastrenko, *Geokhimiya,* **1976**, 803.

4) H. Muraishi, *Am. Mineral.,* **74**, 1147 (1989).

5) H. P. Eugster, *Science,* **157**, 1177 (1967).

6) K. Beneke and G. Lagaly, *Am. Mineral.,* **68**, 818 (1983).

7) B. F. Jones, H. P. Eugster, and S. L. Rettig, *Geochim. Cosmochim. Acta,* **41**, 53 (1977).

8) Y. S. Cherkinskii and I. S. Kuyaz'kova, *Dokl. Akad. Nauk SSSR,* **198**, 358 (1971).

9) H. P. Eugster, *Contrib. Mineral. Petrol.,* **22**, 1 (1969).

10) T. Sasaki, M. Watanabe, Y. Komatsu, and Y. Fujiki, *Inorg. Chem.,* **24**, 2265 (1985).

11) G. Lagaly, German Patent 2742912 (1977).